ARTICLES

Structure and Transport Properties of PEO−$Li_2O·3B_2O_3$ Mixed-Phase Composites

E. Quartarone, P. Mustarelli,* C. Tomasi, and A. Magistris

C.S.T.E.-C.N.R. and Department of Physical Chemistry, University of Pavia, Via Taramelli 16, 27100 Pavia, Italy

Received: February 24, 1998; In Final Form: September 9, 1998

The conductivity of poly(ethylene oxide) (PEO) based electrolytes can be enhanced by addition of ceramic fillers. We study the properties of composite host matrices obtained by adding to PEO a lithium triborate glass prepared by sol−gel. By means of X-ray diffraction and ^{13}C NMR at the magic angle, we show that there is no chemical interaction among the PEO chains and the filler. Lithium cations enter the PEO structure and increase the polymer amorphous phase by creating transient cross-links. The conductivity data are analyzed in terms of the Meyer−Neldel equation.

Introduction

Poly(ethylene oxide) (PEO) based polymer electrolytes have so far been the most studied materials for applications in electrochemical devices.[1] Since the discovery by Armand et al.,[2] various strategies have been followed in order to improve their transport, thermal, and mechanical properties.[3] Among the various approaches that were pursued, special attention has been devoted to the preparation of mixed-phase composite electrolytes[4] that are generally obtained by adding inorganic fillers directly to the PEO−salt solution.

The pioneering work in this field is due to Weston and Steele,[5] who added α-Al_2O_3 to PEO_8−$LiClO_4$ and obtained a substantial improvement of the electrolyte mechanical stability, while the conductivity remained practically unchanged. After that, several mixed-phase composite electrolytes have been studied, both employing conducting fillers such as NASICON,[6] β- and β''-aluminas,[7,8] and ionic glasses,[9] and nonconducting ones such as γ-$LiAlO_2$[10,11] and zeolites.[12] Recently, the use of filler particles in the nanometer range has been shown to allow a substantial increase of the conductivity.[13, 14]

Mixed-phase composite electrolytes are generally constituted of at least three different amorphous or crystalline phases, and the existence of concurrent transport mechanisms (ion hopping and chain-assisted motion),[15] as well as their decoupling with temperature,[16] has been reported. It has been shown that dc conductivity of composite electrolytes may be conveniently described by effective medium theory (EMT) approaches.[17,18] On the other hand, the semiempirical Meyer−Neldel (MN) rule, which requires the conductivity to be Arrhenius-like, also has been demonstrated to be useful in the study of mixed-phase composite electrolytes.[9,19]

However, our overall knowledge of the physicochemical properties of mixed-phase electrolytes is still quite unsatisfactory. It is well accepted that fillers improve the mechanical and electrochemical stability of the electrolyte, the overall interfacial stability of the electrochemical cell,[10,20] and, in general, the electrolyte conductivity by enlarging the PEO amorphous phase.[21,22] On the other hand, the level of interactions among filler, host polymer, and doping salt, such as the different roles that can be played by conducting and nonconducting ceramics, are not yet well understood.[23]

In our previous studies we showed that a room temperature conductivity of $\sim 10^{-5}$ Ω^{-1} cm^{-1} may be easily obtained by adding to the PEO−salt mixture both sodium[24] and lithium[25] triborate glasses prepared according to a sol−gel route. In principle, the presence of the residual organic groups from the sol−gel process was thought to facilitate the intimate mixing of polymer and filler in a common solvent like methanol. However, no relevant differences were found in the bulk properties of composite electrolytes obtained by the filler as-prepared, or subjected to thermal densification treatments that cause the organic groups to leave the glass.

To obtain a deeper insight into the role played by the conducting inorganic fillers and, at the same time, to decouple the contributions of the salt cations from those of the filler itself, we present here a study of the host matrix, without the lithium salt, prepared by mixing PEO and different quantities of $Li_2O·3B_2O_3$ sol−gel glass. The structural modifications that can be induced by the filler on the PEO chains are studied by X-ray diffraction and $^{13}C-^{1}H$ CP-MAS NMR. The correlations between sample amorphicity and dc conductivity are addressed by thermal analysis and impedance spectroscopy.

Experimental Details

Sample Preparation. Lithium triborate ($Li_2O·3B_2O_3$) has been chosen as the hybrid filler. It has been prepared via sol−gel, starting from trimethoxyboroxine (Aldrich) and lithium methoxide (Aldrich), in a dry inert gas atmosphere, as described in detail elsewhere.[26]

Pure powder PEO (BDH Ltd., Polyox WSR-301, MW $\cong 6 \times 10^5$) and the glassy filler have been dried respectively at 55 and 90 °C for 24 h in an oven under primary vacuum (10^{-2} Torr).

* Corresponding author.

10.1021/jp981261m CCC: $15.00
Published on Web 11/10/1998

Mixed-phase composite electrolytes, with 0−50 wt % of filler, were prepared by the casting procedure using anhydrous methanol (Aldrich, <5 ppm of H_2O) as the solvent. PEO was dissolved in methanol and stirred for 2 h. The desired amounts of the glassy lithium triborate were added in the solution and stirred at room temperature for 2 days up to its complete dissolution. These mixtures were cast on Teflon disks in order to slowly evaporate the solvent and then dried under vacuum with the following heating protocol: (1) at 35 °C for 12 h; (2) at 50 °C for 2 days. The obtained films were homogeneous, with a thickness varying in the range 50−250 μm.

Apparatus. DSC measurements were performed on samples of about 20 mg under N_2 purging gas, using a DuPont DSC unit 910. Some of the matrices were studied with a MDSC 2970 (MDSC, TA Instruments). Both DSC 910 and MDSC 2910 are controlled by a 2000 thermal analyzer (TA Instruments).

Powder X-ray diffraction patterns were collected with a Philips PW 1710 powder diffractometer, equipped with a Philips PW 1050 vertical goniometer and a graphite crystal monochromator (Cu Kα radiation).

Impedance spectra were obtained with a Solartron 1255 frequency response analyzer (FRA), in the temperature range 25−150 °C and in the frequency range 1 Hz to 1 MHz. Disk-shaped samples were sandwiched between two silver plates, and the measurements were carried out in a Büchi TO-50 oven under primary vacuum.

NMR spectra were obtained with a AMX400WB (Bruker) spectrometer and a multinuclear MAS probe (Bruker) at 101.6 MHz using the $^{13}C-^{1}H$ cross polarization (CP) MAS technique.[27] The samples were spun at ∼2.5 kHz. A contact time of 5 ms and a 90° pulse of 5.5 μs for the protons were used.

Theoretical Background

If the behavior of the conductivity is Arrhenius, we can obtain information in terms of the Meyer−Neldel (MN) equation[28]

$$\ln A = aE_a + b \tag{1}$$

where A and E_a are the preexponential factor and the activation energy, respectively, which can be extracted from the Arrhenius relation

$$\sigma T = A\, e^{-E_a/(kT)} \tag{2}$$

Although the MN equation has been initially introduced for semiconductors,[28] it was also applied to crystalline and glassy ionic conductors[29,30] and, more recently, to polymer electrolytes.[9,19] Despite some attempts to rationalize it on a thermodynamical basis,[30] however, the MN formalism remains a phenomenological approach for which an atomistic interpretation is lacking. Nowick et al.[31] discussed the limits for which the MN relation is obeyed by ionic conductors.

It may be of interest to detail the approximations we are implicitly making when the MN formalism is used. From the theory of random walk[32] the dc conductivity in a crystalline ionic conductor is given by

$$\sigma T = \frac{Ne^2a^2}{k}\gamma c(1-c)\omega_0\, e^{\Delta S_a/k}\, e^{-E_a/(kT)} \tag{3}$$

where e is the electronic charge, a is the hopping distance, c is the concentration of the mobile ions over N equivalent lattice sites per unit volume, γ is a correlation factor on the order of unity, k is Boltzmann's constant, T is the absolute temperature, ω_0 is the ion vibrational frequency in the potential well, and S_a and E_a are the entropy and energy for conduction, respectively. In terms of the eq 2 the prefactor A takes the form

$$A = \frac{Ne^2a^2}{k}\gamma c(1-c)\omega_0\, e^{\Delta S_a/k} = K\omega_0\, e^{\Delta S_a/k} \tag{4}$$

where K is a carrier concentration factor. By taking the logarithms, we obtain

$$\ln A = \frac{\Delta S_a}{k} + \ln(K\omega_0) \tag{5}$$

which is structurally similar to eq 1. Regarding the approximations we have to make, the difference between a perfect crystal and an amorphous conductor chiefly resides in the entropic factor, and ω_0 is no longer constant but is given by an average over the jumping sites. However, the entropic factor is on the order of 10 for a wide range of systems,[31] whereas ω_0 should not be far from $\sim 10^{13}$ Hz.

A simple relation between the entropy and energy of conduction was proposed by Dienes for atomic diffusion in metals,[33]

$$\Delta S_a = \frac{E_a}{T_f} \tag{6}$$

where T_f is the melting temperature of the metal. This relation was shown to hold for a large number of systems; in particular, it is valid for ionic conductors if T_F is the temperature of an order−disorder transition. At T_f the difference between the free energy of the ions belonging to crystalline and amorphous phases is supposed to be zero.[29] By combining eqs 5 and 6, we obtain the following expressions for the coefficients of eq 1:

$$a = \frac{1}{kT_f}; \quad b = \ln(K\omega_0) \tag{7}$$

To say that a "family of related materials" obey the MN equation therefore means that they must have (i) the same value of T_f and (ii) the same value of $\ln(K\omega_0)$. However, it is generally accepted that a family of materials obeying the MN equation should have a nearly constant value of K.[4,29,31] As a consequence, the order-of-magnitude variations of A that are usually observed are chiefly determined by entropy and/or enthalpy of migration. Similar conclusions were drawn by Wieczorek et al. about their ternary composite polymer electrolytes.[9,34]

In the already cited paper,[31] Nowick et al. proposed an alternative formulation of the MN equation:

$$\ln\left(\frac{A}{A_{ref}}\right) = \frac{E_a}{kT_0} - \frac{H_m}{kT_0} \tag{8}$$

Here, H_m is the enthalpy of migration, A_{ref} is the prefactor in a temperature region where all the cations are free to move ($E_a = H_m$), and T_0 has nearly the same meaning as T_f. This new formulation allows us to obtain both T_0 and H_m from the intercept of $\ln(A/A_{ref})$ vs E_a. It differs from eq 1 chiefly because A_{ref} contains the concentration term $c(1-c)$ that depends on the sample. However, the quantity $\ln[c(1-c)]$ should not change appreciably over the composition series, so the differences from eq 1 are negligible. The authors state that the key assumptions, and hence the limits, of their model are that H_m and T_0 must be constant over the whole range of compositions

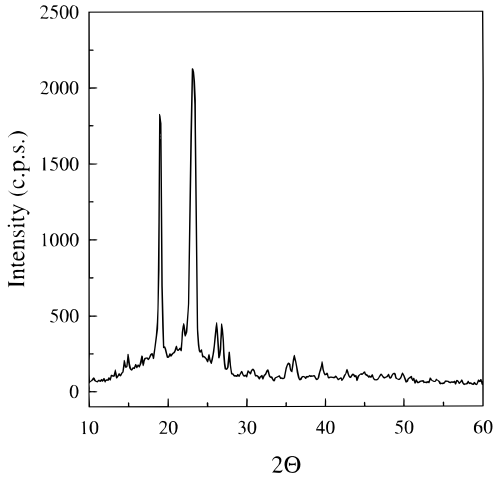

Figure 1. X-ray diffractogram of a film of pure PEO.

that make up the family of materials being considered. This assumption may be quite restrictive if a wide range of compositions is covered.

Results

X-ray Diffraction. Figure 1 shows the diffractogram of a pure PEO film obtained by a standard casting procedure. The most relevant features are a narrow peak at $2\theta = 18.98°$ (0,2,1 Miller indices) and a large, unresolved, manifold centered at $2\theta = 23.10°$ (2,3,0 Miller indices). The results are in substantial agreement with the structural data on crystalline PEO reported in 1973 by Takahashi and Takodoro.[35] The filler addition does not determine clear trends either in the main reflection positions or in their widths except for a generalized 30% increase of the manifold width near 23°, which can be accounted for in terms of (i) the presence of small spherulites formed after the addition of the filler or (ii) the long-range disorder introduced by the ionic glass. The former possibility is somehow also supported by the small average decrease of the polymer melting temperature T_m (see DSC section and Table 1).

Figure 2 shows the behavior of the peak positions vs the filler content, expressed both as a weight fraction and in terms of the ratio $n = [O]/[Li]$. The relatively high dispersion observed at higher angles is likely due to the presence of an unresolved manifold. This simple analysis shows that the filler addition does not modify the crystalline structure of PEO by forming a PEO−glass complex, despite the presence in the sol−gel glass of residual CH_3O- organic groups.

^{13}C CP-MAS NMR. Figure 3 shows the chemical shift positions of the secondary carbons of the PEO chains vs filler concentration. The addition of the filler causes a nearly constant paramagnetic shift of ∼0.1 ppm with respect to the position of

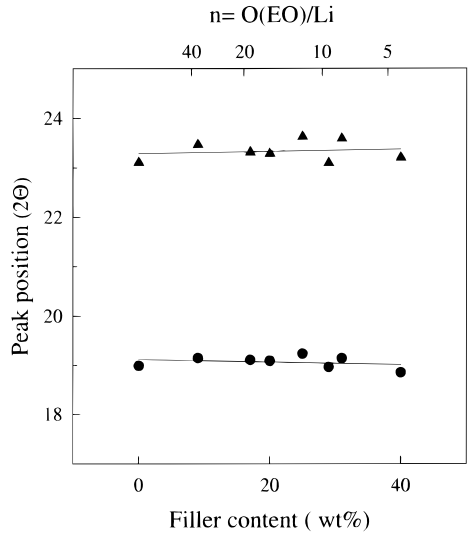

Figure 2. Positions of the two main peaks of Figure 1 vs the filler content, expressed both as weight fraction and in terms of the ratio $n = [O]/[Li]$.

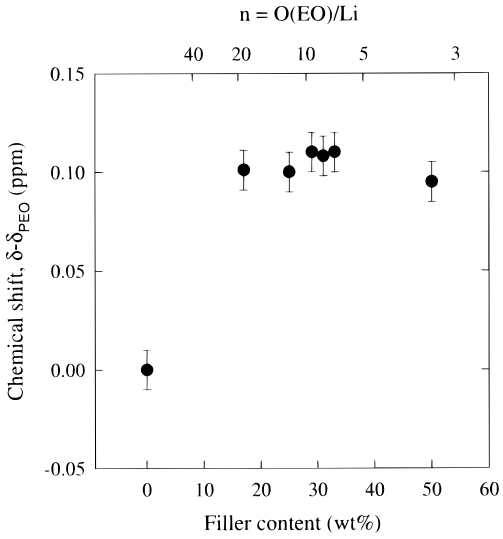

Figure 3. ^{13}C NMR chemical shift positions of the secondary carbons of the PEO chains vs filler concentration.

the chain carbons in pure PEO. We can attribute this shift to the inductive effect caused by the lithium ions coordinated with the ether oxygens, which are somehow "seen" by the secondary carbons. A shift of 0.1 ppm corresponds to ∼10 Hz, which is a reasonable value in terms of the lithium electropositivity.[36] As a consequence, we have again no evidence of chemical interactions among the PEO chains and the glassy filler.

DSC. Figure 4 shows the DSC thermograms of pure PEO

TABLE 1

sample (filler wt %)	O(EO)/ Li	T_m (K)	σ_{rt} (Ω^{-1} cm^{-1})	E_a; $T < T_m$ (eV)	E_a; $T > T_m$ (eV)	ln A; $T < T_m$ (Ω^{-1} K cm^{-1})	ln A; $T > T_m$ (Ω^{-1} K cm^{-1})
0		339	1.99×10^{-10}	0.98	0.21	21.9	−2.5
9	37.6:1	331	6.31×10^{-10}	0.96	0.32	19.7	4.6
17	18.8:1	331	4.26×10^{-10}	0.87	0.30	18.4	3.4
20	15:1	332	2.25×10^{-10}	1.02	0.43	23.4	9.0
25	11.3:1	328	1.20×10^{-9}	0.88	0.39	19.3	6.9
29	9.4:1	331	6.76×10^{-10}	0.88	0.36	18.9	5.5
31	8.5:1	339	1.55×10^{-9}	0.83	0.54	17.4	9.9
33	7.5:1	336	2.00×10^{-9}	0.87	0.48	18.5	8.3
36	6.6:1	333	1.25×10^{-9}	0.94	0.50	21.0	8.3
40	5.6:1	331	2.29×10^{-10}	0.85	0.35	16.5	4.3
50	3.8:1	328	3.23×10^{-10}	1.05	0.32	23.8	3.5

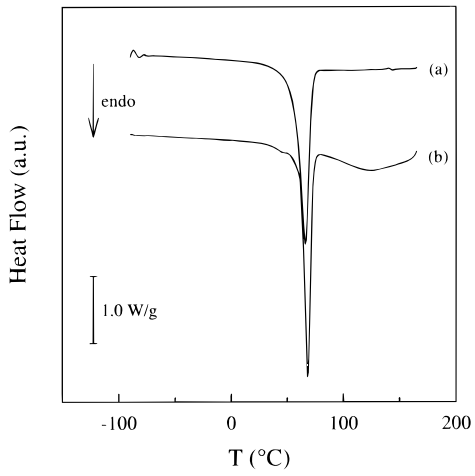

Figure 4. DSC thermograms of pure PEO (a) and of the PEO−$Li_2O{\cdot}3B_2O_3$ composite with 33 wt % of filler (b).

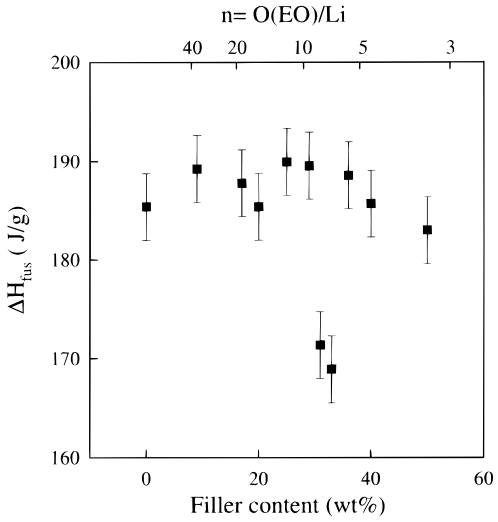

Figure 5. Specific melting enthalpy ΔH_m of the composite films vs the filler concentration. An uncertainty of ± 3.5 J g^{-1} is estimated.

(curve a) and of the PEO−$Li_2O{\cdot}3B_2O_3$ composite with 33 wt % of filler (curve b). The deep endotherm at 65 °C is due to the melting of the PEO crystalline part. The values of T_m for the different samples are reported in Table 1. From the specific melting enthalpy of curve a, $\Delta H_m = 185.4$ J g^{-1}, we find that our pure PEO film has a crystallinity $X_c \cong 87\%$. In fact, $\Delta H_m = 213.5$ J g^{-1} has been reported for completely crystalline PEO.[9]

Curve b shows an endotherm similar to that of pure PEO and, in addition, a second endotherm between 80 and 160 °C. This last feature is not observed in all the other samples except, at a lower extent, in the one containing 31 wt % of filler. It can be likely assigned to the endothermic mixing between the crystalline PEO chains that underwent melting at 65 °C and the metastable liquid phase originating at the polymer glass transition. The relevance of this endotherm suggests that the composite with 33 wt % of filler may contain a larger amorphous fraction than pure PEO or the other compositions. This is confirmed by plotting the values of ΔH_m vs the filler concentration, as shown in Figure 5. We observe that, in general, ΔH_m spans the range 183−189 J g^{-1}. Considering a 2% of uncertainty in the peak integration, this means that the PEO crystalline fraction of the studied systems remains practically constant for filler content in the range 0−29 and 36−50 wt %. The samples with 33 wt % and 31 wt % of filler display

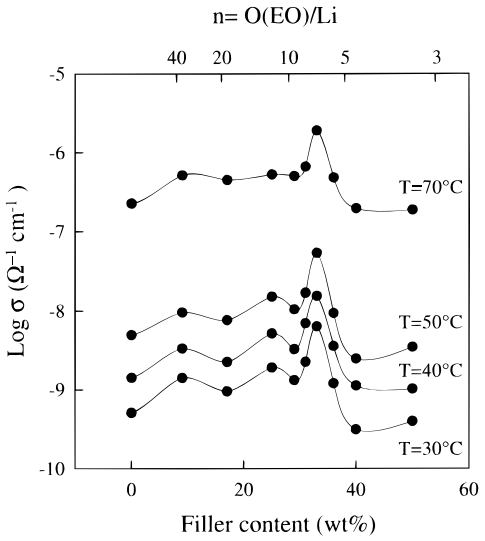

Figure 6. Behavior of conductivity at different temperatures vs the filler content.

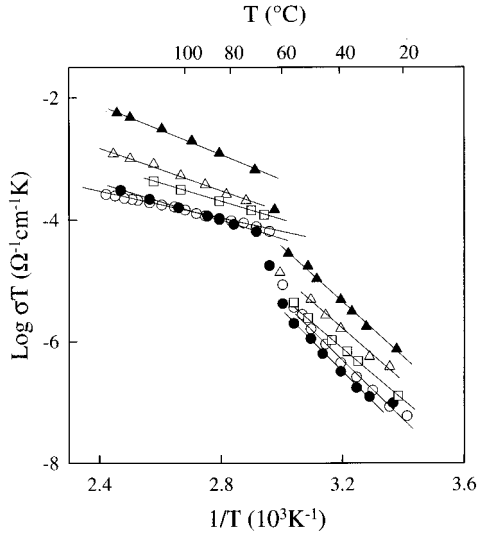

Figure 7. Behavior of conductivity vs reciprocal temperature for pure PEO (open circles) and matrices with different filler content: 17 wt % (open squares), 25 wt % (open triangles), 33 wt % (filled triangles), and 50 wt % (filled circles). The lines are linear best fits.

ΔH_m minima of 168 J g^{-1} and 171 J g^{-1}, respectively, which correspond to a polymer crystallinity of $X_c \cong 78\%$.

Conductivity Data. For all the samples a single and depressed semicircle was obtained at each temperature by impedance spectroscopy measurements. Figure 6 shows the behavior of the conductivity at different temperatures vs the filler content. At each temperature a maximum is found for ∼33 wt % of filler content, which is nearly at the same composition where the minimum PEO crystal fraction is found. At lower filler concentration, conductivity values slightly higher than those of pure PEO are observed, whereas the conductivity drops by nearly 1 order of magnitude when the glass content reaches 40−50 wt % of the total. This can be likely explained by considering the progressive dilution effect of the amorphous polymer phase[10] that after a certain limit begins to act as just a binder [37] for the less-conductive glass grains. In fact, the room temperature conductivity of triborate glass is on the order of 10^{-12} Ω^{-1} cm^{-1}.[25]

Figure 7 shows the behavior of the conductivity vs the reciprocal temperature for pure PEO and for samples with different filler content. For all the matrices we studied, the

conductivity displays a sigmoidal shape around the T_m of PEO that can be approximated by two Arrhenius curves with different activation energies below and above the PEO melting. As expected, however, the samples containing ~33 wt % of filler are characterized by less abrupt conductivity changes in correspondence to the T_m.

Discussion

Filler Contribution to the Structure. The combined evidence of our spectroscopic and diffractometric data demonstrates that no interactions exist between PEO and the glassy filler. At the same time, however, DSC analysis shows that a minimum of the crystallinity is obtained at near ~33 wt % of the filler content (see Figure 5). This minimum, which corresponds to the highest conductivity we observed, is well defined and relatively narrow. As a comparison, Wieczorek reported a monotonic decrease and an oscillating behavior of X_c for the systems $(PEO)_{10}-LiClO_4-(Li_2O-B_2O_3-SiO_2)$ and $(PEO)_{10}-LiClO_4-$ionite, respectively.[9]

In PEO−salt−filler ternary systems, conductivity maxima are generally found near 10−15 wt % of filler content.[9,10] It is well accepted that these maxima are caused by the combined effect of (i) an enlarged amorphous phase related to filler steric hindrance and (ii) a dilution process that reduces the volume available for the PEO chain-assisted transport. In the case of the binary system we are examining, different considerations should be made.

It was earlier shown[38] that lithium cations play the role of cross-linking agents among the PEO chains. In particular, when $LiClO_4$ is used as the doping salt, the conductivity tends to level off at a critical salt concentration that corresponds to a chain length of ~12 EO units between two Li^+ ions; anion reassociation and complex formation take place for higher salt concentrations. Moreover, the phase diagrams of the systems PEO−LiX generally display eutectics in the range $8 \leq O(EO)/Li \leq 20$.[39−41] Anomalies of ^1H, ^7Li, and ^{13}C NMR line widths and longitudinal relaxation times for $5 < O(EO)/Li < 10$ have been recently reported on the system PEO−poly(epichloridrine)−$LiClO_4$.[42]

We can pictorially represent our composite materials as constituted of a dispersion of filler particles surrounded by an interphase made of both crystalline and amorphous PEO chains. A fraction of the lithium cations (likely those near the surface of the filler particles) will be solvated by the two PEO phases depending on their different dielectric constants, i.e., $\epsilon \approx 7.8$ [43] for the amorphous PEO and $\epsilon \approx 4$ for the crystalline one. The fraction of cations available for the solvation is roughly related to the particle dimension through their surface-to-volume ratio. When the filler content becomes large enough to ensure that the PEO interphase can solvate a suitable number of Li^+ cations, a maximum of the amorphous fraction is found that corresponds to the observed maximum of the conductivity. This happens when ~33 wt % of glassy filler is added to the pure PEO. In other words, we suppose that our glassy filler behaves like a conventional lithium salt from the point of view of PEO−cation interactions. In contrast, the borate macroanions are dispersed in the host matrix and remain chemically isolated from the polymer chains. Preliminar hot-stage polarizing microscopy experiments seem to indicate that the characteristic length of the dispersion is in the submicrometer range. This conclusion is in substantial agreement with our NMR, DSC, and conductivity data.

As a matter of fact, the conductivity anomaly near 33 wt % of filler content may be also explained by invoking an optimum ratio in terms of particles size and/or connectivity between the PEO matrix and the filler dispersion. However, this possibility is unlikely because it would imply that a grain-boundary-assisted transport mechanism is exclusive or predominant in determining the ionic conductivity, which is not the case as demonstrated by the jump of σ near the PEO melting temperature (see Figure 7).

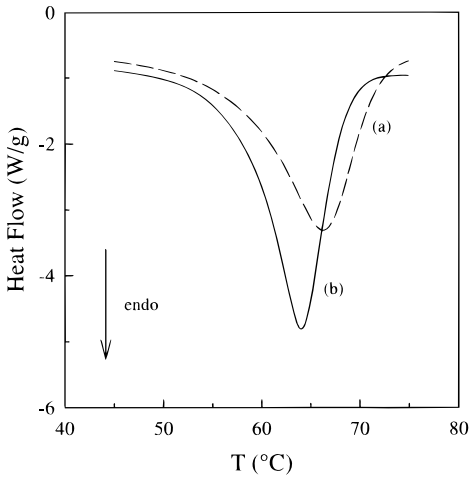

Figure 8. DSC thermograms of pure PEO (a) and of the PEO−$Li_2O{\cdot}3B_2O_3$ composite with 44 wt % of filler (b). The figure shows the temperature region around the PEO melting temperature T_m.

For a filler content of ~40 wt % or higher, a new crystalline complex probably begins to form, according to the data reported in the literature.[40,44] This may account for the new crystallinity increase monitored by DSC (see Figure 5). A subtle confirmation in this sense may be obtained by a careful comparison of the DSC melting endotherms of pure PEO and the film containing 40 wt % of filler (1.5:1 sample), which are shown in Figure 8. The peak of the sample 1.5:1 is downshifted by about 10 °C, and its shape is quite different from that of pure PEO. We can consider the endotherm of 1.5:1 as due to the melting of a complex and/or to the eutectic between the complex itself and pure PEO. However, the crystallites of the new complex must be very small, since we do not have evidence for them in our X-ray diffraction patterns.

Finally, we do not have evidence of chemical interactions between the polymer chains and the organic groups coming from the sol−gel preparation of the glassy filler. Of course, we recognize that there could exist microstructural or transport differences among mixed-phase systems obtained from a common solvent, or by simple dispersion of the filler in the host polymer. This analysis, however, has not been performed in the present work.

Filler Contribution to the Conductivity. Figure 9 shows the plot of the values of $\ln A$ vs E_a extracted from the conductivity data both below and above the PEO melting temperature (see Table 1). By fitting the data with eq 1, we obtain $T_f \cong 445 \pm 12$ K. We stress that the values of E_a and $\ln A$ of pure PEO have not been used in the fitting procedure because PEO is an insulating material, and as such, it cannot be considered "related" to the Li^+ conducting mixed-phase composites.

The fact that the conductivity data both below and above T_m are well fitted by the same MN equation is an indication that the transport mechanism does not change across the PEO melting. Concerning the physical meaning of the parameter T_f, we recall that, for PEO-based systems, it is usually put into relation with the crystalline PEO melting temperature T_m.[4]

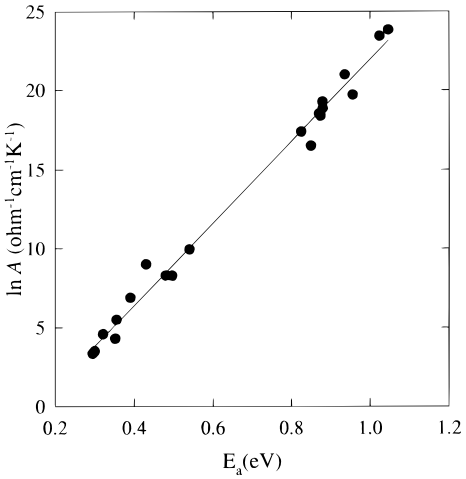

Figure 9. MN plot of the prefactors vs the activation energies extracted by linear best fits of the conductivity data both below and above the PEO melting temperature.

However, the value we obtained from the MN fit is substantially higher than T_m. The general case $T_f > T_m$ can be accounted for by considering that filler addition improves the micromechanical properties of the PEO film in such a way that a thermal activation is needed to equalize the chemical potentials of the ions belonging to the preexistent polymer amorphous phase and to the one formed above the PEO melting. In fact, following the thermodynamic model suggested by Wieczorek,[34] we have

$$\mu_{ia}(T_g) - \int_{T_g}^{T_m} S_{ia}\,dT - \int_{T_m}^{T_f} S_{ia}\,dT = \mu_{ic}(T_g) - \int_{T_g}^{T_m} S_{1ic}\,dT - \int_{T_m}^{T_f} S_{2ic}\,dT \quad (9)$$

where μ_{ia} and μ_{ic} are the chemical potentials of the ith ionic species belonging to the amorphous and crystalline phases, respectively. S_{1ic} and S_{2ic} are the partial molar entropies of the ith ionic species in the crystalline phase below and above T_m, respectively, and S_{ia} is the partial molar entropy in the amorphous phase. If we assume that $S_{2ic} = S_{ia}$ (as it is reasonable for amorphous phases having the same viscosity), we obtain $\mu_{ia}(T_m) = \mu_{ic}(T_m)$ and hence $T_f = T_m$. For systems in which $S_{2ic} \neq S_{ia}$, if both S_{2ic} and S_{ia} are constant in the temperature range between T_m and T_f, we obtain

$$T_f = T_m + \frac{\mu_{ic}(T_m) - \mu_{ia}(T_m)}{S_{2ic} - S_{ia}} \quad (10)$$

which may account for the difference between the values of T_f and the T_m of PEO.

Owing to the large difference between T_f and T_m, however, we can try to correlate the T_f value to the completion of the mixing process of the PEO chains belonging to the two different amorphous phases that exist above the PEO melting. This is in agreement with the broad DSC endotherm observed in the range 80−160 °C (see Figure 4b), which is maximum when the ratio between the crystalline and the amorphous PEO phases goes toward the unity, i.e., for the samples near 33 wt % of filler (see Figure 5). However, we recognize that this hypothesis is not graphically supported by the Arrhenius behavior reported in Figure 7. In fact, to obey the MN relation, there should be a temperature range in which the conductivity curves overlap, which does not seem to be the case for the points of Figure 7 above 400 K.

The concept of an order−disorder transition taking place well above the PEO melting may be further explored by reconsidering our data in terms of the formalism of Nowick et al.[31] We can suppose that our samples belong to the extrinsic associated range (stage III) below the PEO melting, whereas a transition to the extrinsic dissociated range (stage II) takes place somewhere above that temperature. In stage II, all the cations are thought to be free and we have $E_a = H_m$, and $A \cong A_{ref}$ (see eq 8 and related discussion). In stage III almost all carriers are bound, and only those that are released can contribute to the conductivity. The number of carriers participating to the conduction is strongly activated, and we have

$$E_a = H_m + \Delta H \quad (11)$$

where ΔH is the enthalpy for defect formation. In the case of dilute systems, moreover, we have $A \gg A_{ref}$. This is the case for our samples, as can be seen in Table 1. If we fit our data in terms of the eq 8 by taking $A_{T>T_m} \cong A_{ref}$, we obtain $H_m = 0.30$ eV and $T_0 = 470$ K. We observe that H_m is in reasonable agreement with the values of E_a for $T > T_m$, except for filler contents near 33 wt % (see Table 1), and that T_0 is not greatly different from T_f.

The combined evidence of eqs 1 and 8 suggests the following overall model for the ionic conductivity in our PEO-based composites. As stated in the previous section, some of the filler cations are solvated by both the crystalline and amorphous PEO chains. As expected, however, only the cations belonging to the PEO amorphous part will contribute to the transport. The resulting conductivity is strongly activated ($E_a \approx 1$ eV), and the prefactor is very high ($A \approx 10^9-10^{10}$ Ω^{-1} K cm^{-1}) as expected for diluted systems.

Above the PEO melting, on the other hand, we can assume that nearly all the cations in the PEO phase(s) will contribute to the transport. By extrapolating the high-temperature conductivity below T_m (see Figure 7), we may deduce that the fraction of carriers is reduced to ∼10% immediately below the PEO melting and to ∼1% near room temperature. The cation transition from the "bound" state to the "free" one is controlled by the mixing of the PEO chains of the different liquid phases. Only when the mixing process has been completed the system is at equilibrium, and all the cations are free to move (stage II in the scheme of Nowick et al.). In this sense, both T_f and T_0 seem to indicate the temperature of the transition between stages II and III. The determination of T_0, however, is affected by a large uncertainty because the best fit of eq 8 is performed under the approximation $A_{ref} \cong A_{T>T_m}$.

For $T > T_m$ the activation energy for the conductivity, E_a, substantially coincides with the enthalpy of migration H_m. The large discrepancies observed for filler content between 30 and 40 wt % may be accounted for by considering that the larger the PEO amorphous fraction is, the more relevant the mixing process is. Since the values of E_a are obtained immediately above T_m, it is reasonable to suppose that they still retain some contributions from the enthalpy of defect formation. From eq 11 we obtain $\Delta H \approx 0.6-0.7$ eV at $T < T_m$, which is in agreement with some data reported on the system PEO−NaI−θ-Al_2O_3.[4]

We cannot fully rule out the possibility that a grain-assisted transport mechanism contributes to the overall ionic conductivity both below and above the PEO melting temperature. However, if present, this contribution should be minor with respect to the usual ionic motion assisted by the PEO chains.

Conclusions

We studied by a number of techniques the structural, thermal, and transport properties of composite host matrices for solid-state polymer electrolytes. Our overall findings allow us to depict the following model for the structure and the transport properties of our composite matrices.

(1) Sol−gel glassy filler does not interact with PEO and does not modify the structure of its crystalline part.

(2) A fraction of the filler Li^+ ions enter the PEO structure in a way that is similar to what happens in the PEO−salt solvent-free polymer electrolytes. The cations form transient cross-links with the PEO chains.

(3) According to the literature, the transport takes place in the PEO amorphous phase. Immediately below T_m the fraction of Li^+ ions participating in the conduction is on the order of 10% of those solvated by PEO. Above T_m nearly all the cations contribute to the conductivity, but the transition toward the "free ion" regime is controlled by the mixing of the PEO chains.

Acknowledgment. This research has been partially funded by Progetto Strategico "Batterie Leggere" of the Italian CNR. The paper is part of the Ph.D. work of E.Q.

References and Notes

(1) Armand, M. B. *Solid State Ionics* **1994**, *69*, 309.
(2) Armand, M. B.; Chabagno, J. M.; Duclot, M. *Fast Ion Transport in Solids*; Elsevier: New York, 1979; p 131.
(3) See, for example, the following. Linford, R. G. *Applications of Electroactive Polymers*; Chapman & Hall: London, 1993; p 1.
(4) Wieczorek, W. *Composite Polyether Based Electrolytes*; Oficyna Wydawnicza Politechniki Warszawskiej: Warszawa, 1995 (in English).
(5) Weston, J.; Steele, B. C. H. *Solid State Ionics* **1982**, *7*, 75.
(6) Plocharski, J.; Wieczorek, W. *Solid State Ionics* **1988**, *28−30*, 979.
(7) Wieczorek, W.; Such, K.; Przyluski, J.; Florjanczyk, Z. *Synth. Met.* **1991**, *45*, 373.
(8) Croce, F.; Bonino, F.; Panero, S.; Scrosati, B. *Philos. Mag. B* **1989**, *59*, 161.
(9) Wieczorek, W. *Mater. Sci. Eng.* **1992**, *B15*, 108.
(10) Capuano, F.; Croce, F.; Scrosati. B. *J. Electrochem. Soc.* **1991**, *138*, 1918.
(11) Borghini, M. C.; Mastragostino, M.; Passerini, S.; Scrosati, B. *J. Electrochem. Soc*. **1995**, *142*, 2118.
(12) Croce, F.; Scrosati, B. *J. Power Sources* **1993**, *43−44*, 9.
(13) Nagasubramanian, G.; Attia, A. I.; Halpert G.; Peled, E. *Solid State Ionics* **1993**, *67*, 51.
(14) Matsuo, Y.; Kuwano, J. *Solid State Ionics* **1995**, *79*, 295.
(15) Kumar, B.; Weissman, P. T.; Marsh, R. A. *J. Electrochem. Soc*. **1993**, *140*, 321.
(16) Wieczorek, W.; Chung, S. H.; Stevens, J. R. *J. Polym. Sci., Part B: Polym. Phys*. **1996**, *34*, 2911.
(17) Wieczorek, W.; Such, K.; Florjanczyk, Z.; Stevens, J. R. *J. Phys. Chem*. **1994**, *98*, 6840.
(18) Wieczorek, W.; Such, K.; Chung, S. H.; Stevens, J. R. *J. Phys. Chem*. **1994**, *98*, 9047.
(19) Wieczorek, W.; Such, K.; Plocharski, J.; Przyluski, J. *Proceedings of the Second International Symposium on Polymer Electrolytes*; Elsevier: London, 1990; p 339.
(20) Croce, F.; Capuano, F.; Selvaggi, A.; Scrosati, B. *J. Power Sources* **1990**, *32*, 389.
(21) Wieczorek, W.; Such, K.; Wycislik, H.; Plocharski, J. *Solid State Ionics* **1989**, *36*, 255.
(22) Croce, F.; Scrosati, B.; Mariotto, G. *Chem. Mater*. **1992**, *4*, 1134.
(23) Quartarone, E.; Mustarelli, P.; Magistris, A. *Solid State Ionics* **1998**, *110*, 1.
(24) Magistris, A.; Ferloni, P.; Mustarelli, P.; Restelli, M.; Chiodelli, G. *Solid State Ionic Materials*; World Scientific: Singapore, 1994; p 361.
(25) Mustarelli, P.; Quartarone, E.; Tomasi, C.; Magistris, A. *Solid State Ionics* **1996**, *86−88*, 347.
(26) Mustarelli, P.; Quartarone, E.; Tomasi, C.; Magistris, A. *J. Non-Cryst. Solids* **1997**, *215*, 51.
(27) See, for example, the following. Fyfe, C. *Solid State NMR for Chemists*; C.F.C. Press: Guelph, Ontario, 1983; p 268.
(28) Meyer, W.; Neldel, H. *Z. Tech. Phys*. **1937**, *12*, 588.
(29) Almond, D. P.; West, A. R. *Solid State Ionics* **1986**, *18−19*, 1105.
(30) Almond, D. P.; West, A. R. *Solid State Ionics* **1987**, *23*, 27.
(31) Nowick, A. S.; Lee, W.-K.; Jain, H. *Solid State Ionics* **1988**, *28−30*, 89.
(32) Huggins, R. A. *Diffusion in Solids, Recent Developments*; Academic Press: London, 1975; p 445.
(33) Dienes, G. J. *J. Appl. Phys*. **1950**, *21*, 1189.
(34) Wieczorek, W. *Solid State Ionics* **1992**, *53−56*, 1064.
(35) Takahashi, Y.; Takodoro, H. *Macromolecules* **1973**, *6*, 672.
(36) See, for example, the following. Friebolin, H. *Basic One- and Two-Dimensional NMR Spectroscopy*; VCH: Weinheim, 1993; p 96.
(37) Skaarup, S.; West, K.; Zachau-Christiansen, B. *Solid State Ionics* **1988**, *28−30*, 975.
(38) Cheradame, H.; Le Nest, J. F. *Polymer Electrolyte Reviews*; Elsevier Applied Science: London, 1987; Vol. 1, p 103.
(39) Ferloni, P.; Chiodelli, G.; Magistris, A.; Sanesi, M. *Solid State Ionics* **1986**, *18−19*, 265.
(40) Fauteux, D. *Polymer Electrolyte Reviews*; Elsevier Applied Science: London, 1989; Vol. 2, p 121.
(41) Vallée, A.; Besner, S.; Prud'homme, J. *Electrochim. Acta* **1992**, *37*, 1579.
(42) Wolfenson, A. E.; Torresi, R. M.; Bonagamba, T. J.; De Paoli, M. A.; Panepucci, H. *J. Phys. Chem. B* **1997**, *101*, 3469.
(43) Porter, C. H.; Boyd, R. H. *Macromolecules* **1971**, *4*, 589.
(44) Wright, P. V. *Polymer Electrolyte Reviews*; Elsevier Applied Science: London, 1989; Vol. 2, p 61.